THE ASTROPHYSICAL JOURNAL, 360:41–54, 1990 September 1

VLA OBSERVATIONS OF THE RADIO GALAXY HYDRA A (3C 218)

G. B. TAYLOR
Department of Astronomy, University of California, Los Angeles and National Radio Astronomy Observatory, Socorro
R. A. PERLEY
National Radio Astronomy Observatory, Socorro
M. INOUE
Nobeyama Radio Observatory, Japan
T. KATO AND H. TABARA
Utsunomiya University, Japan
AND
K. AIZU
Rikkyo University, Japan
Received 1989 November 27; accepted 1990 March 2

ABSTRACT

We present multiconfiguration, multifrequency observations of the radio galaxy Hydra A (3C 218) using the VLA. The radio emission of Hydra A consists of two components: (1) a pair of well-collimated, curved jets possessing "S" symmetry, each of which makes a turn through $\sim 40°$ between the core and the lobe, and (2) diffuse radio lobes, also rotation-symmetric, although straighter, which extend north out to 5′ (420 kpc) and south out to 3′ (250 kpc). The overall morphology of Hydra A is similar to that of wide-angle tail sources.

By combining data taken with the VLA in its A-, B-, C-, and D-configurations, we have made 6 and 2 cm maps with a resolution of 0″.6, allowing for the first time a detailed mapping of the Faraday rotation measure (RM) structure. We find RMs ranging from -1000 to $+3300$ radians m^{-2} in the northern lobe with gradients in the RM of up to 1000 radians m^{-2} arcsec^{-1}. In the southern lobe the gradients in RM are so large that the 6 cm data have been beamwidth-depolarized to less than 2%. This, and the presence of $n\pi$ ambiguities in the remaining polarization-angle data, suggest RMs in excess of ± 3750 radians m^{-2}, the maximum value that we can unambiguously determine.

Subject headings: galaxies: individual (3C 218) — galaxies: jets — interferometry — radio sources: galaxies

I. INTRODUCTION

Extragalactic radio sources have now been detected with widely different morphologies (see reviews by Miley 1980 and Bridle and Perley 1984). Some of the most striking of these are high-luminosity radio galaxies, such as Cygnus A (Perley, Dreher, and Cowan 1984), and Hydra A. With a detailed study of a particular source, we can hope to obtain an understanding of its physical nature and thereby gain insight into the class of extragalactic radio sources as a whole. Radio galaxies also serve as a probe of their environments, providing a means to estimate the pressures, densities, temperatures, and magnetic field strengths of the intergalactic medium (IGM) or intracluster medium (ICM). In this paper we report on an extensive series of observations of the radio galaxy Hydra A using the Very Large Array (VLA) of the National Radio Astronomy Observatory.[1]

In the following sections observations of Hydra A are reported, and the resulting picture of the physical nature of Hydra A is discussed in § IX. Particular attention will be paid to the observed rotation measure (RM) structure, which can provide information about the magnetic fields in and around Hydra A. Studies of extended RMs require high-resolution observations at three or more frequencies, and consequently have been carried out for only a handful of sources to date.

[1] The National Radio Astronomy Observatory is operated by Associated Universities, Inc., under National Science Foundation Cooperative Agreement no. AST-8814515.

II. PREVIOUS OBSERVATIONS OF HYDRA A

a) Radio Observations

Hydra A has long been known as one of the most prominent extragalactic radio sources; it has the seventh highest flux density in the 3C catalog. Its position near the celestial equator ($\delta = -11°53'$) and primarily north-south extent has made high-resolution mapping of it difficult with east-west interferometers. It was mapped with the Owens Valley Radio Observatory twin-element interferometer as part of a survey of extragalactic radio sources by Fomalont (1971) at 1425 MHz with a resolution of 45″. Only the inner 2′ of Hydra A were seen as an elliptical "core-halo" type source with a position angle of 37°.

Ekers and Simkin (1983) observed Hydra A with the Fleurs Synthesis Telescope at 1415 MHz. At their resolution of 50″, however, they were unable to resolve the "S" symmetry of Hydra A, and classified it as a head-tail source. In addition, they observed emission extending as far as 240″ south of the core, but none more than 60″ north of the core.

Kato *et al.* (1987) used the Nobeyama 45 m telescope to survey 100 radio galaxies suspected from depolarization observations to have large RMs, and found four with an integrated RM greater than 1000 radians m^{-2} in absolute value: 3C 119, 3C 147, Hydra A, and 3C 295. Of these four, 3C 119 and 3C 147 are pointlike QSOs, but both Hydra A (this paper) and 3C 295 (Perley and Taylor 1990) have extended structure that can be mapped with the VLA. The finding of such a large integrated RM for Hydra A by Kato *et al.* motivated this study.

As part of a study of optical emission lines in radio galaxies, Baum *et al.* (1988) observed Hydra A with the VLA in the A-, B-, and C-configurations at 2, 6, and 20 cm. Baum *et al.* remarked upon "S" symmetry of the radio lobes of Hydra A, and measured an increasing spectral index with $\alpha = 1.8$ between 6 and 20 cm at the ends of the lobes. Between 2 and 6 cm Baum *et al.* measured minimum RMs of 430 radians m^{-2}.

b) *Optical*

Matthews, Morgan, and Schmidt (1964) described the optical galaxy associated with Hydra A as a cD2 galaxy (Morgan 1958) with an unresolved double nucleus. The position angle of the 24.5 mag $arcsec^{-2}$ isophote is given by Owen and Laing (1989) to be 50°.

Hydra A is $\sim 13'$ (1.1 Mpc)[2] distant from the center of Abell cluster 780 (Abell 1958). Sandage and Hardy (1973) had previously classified Hydra A as the dominant member of a poor, Abell richness 0 cluster which they designated 0915−11, but given that clusters are often irregular in shape, and since the Abell cluster radius is ~ 3 Mpc, we consider it likely that Hydra A belongs to Abell 780. Furthermore, since the X-ray emission (David *et al.* 1990) is centered on Hydra A, it is likely that the true center of A780 is at Hydra A.

The angular size of the Hydra A galaxy was estimated by Sandage and Hardy (1973) from the Palomar Sky Survey prints to be 53″.7 (75 kpc). A deep CCD image of Hydra A reveals a power-law light distribution extending out 72″ (100 kpc) in radius to the 24.5 mag $arcsec^{-2}$ isophote (Owen and Laing 1989). The absolute visual magnitude calculated by Sandage (1973) for Hydra A is $M_V = -23.74$, quite similar to that of other powerful radio galaxies like Cygnus A. The optical data on Hydra A are summarized in Table 1.

Simkin (1979) measured two optical emission lines in the nucleus of Hydra A and found an axis of rotation of $29° \pm 9°$, similar to the radio axis of 37° found by Fomalont (1971). Ekers and Simkin (1983) observed the secondary nucleus to lie at about 10″ (14 kpc) from the primary nucleus at a position angle of 125°.

[2] Throughout this paper we take $H_0 = 50$ km s^{-1} Mpc^{-1}.

TABLE 1

OPTICAL PARAMETERS FOR HYDRA A[a]

Parameter	Value	Reference
Abell cluster	780	1
Abell richness	0	1
Morphological type	cD2	2
Redshift	0.053	3
Distance	322 Mpc	
Linear scale for 1″	1.4 kpc	
m_B[b]	14.58	4
m_V[b]	13.73	4
M_V	−23.74	
Optical core:		
α(1950)	$9^h15^m41^s.20$	5
δ(1950)	11°53′04″.9	5
l(1950)	242°.93	5
b(1950)	25°.095	5

[a] $H_0 = 50$ km s^{-1} Mpc^{-1}.

[b] These apparent magnitudes were calculated to the 26 mag $arcsec^{-2}$ isophote in the $z = 0$ limit.

REFERENCES.—(1) Abell 1958; (2) Matthews, Morgan, and Schmidt 1964; (3) Ekers and Simkin 1983; (4) Sandage 1973; (5) Baum *et al.* 1988.

c) *X-Ray*

Hydra A was observed with the *Einstein* imaging proportional counter (IPC) and monitor proportional counter (MPC), and the results were presented by David *et al.* (1990). They found diffuse emission out to 1 Mpc from the cluster center producing a total luminosity in the X-ray of 4.1×10^{44} ergs s^{-1} between 0.5 and 4.5 keV. This emission is well modeled by thermal bremsstrahlung from an isothermal plasma at 4.5 ± 0.7 keV with a density profile of the form (eq. [1] of David *et al.*)

$$\rho(r) = \rho_0 \left[1 + \left(\frac{r}{a}\right)^2\right]^{-3\beta/2} , \qquad (1)$$

where

$$a = \text{Core radius} = 110'' \; (0.15 \text{ Mpc}) ,$$

$$\beta = \frac{\text{Energy per unit mass in galaxies}}{\text{Specific internal energy of the gas}} = 0.7 ,$$

and r is the distance from the core. Equation (1) matches the observations well only when omitting the central 1′.5 region, where there is a noticeable X-ray excess. This model gives a central hydrogen density of $n_H = 0.0065$ cm^{-3}. The central X-ray excess, which has angular size similar to the IPC resolution, could be produced by an unresolved nuclear component. In general, the X-ray emission associated with Hydra A appears quite similar to that associated with Cygnus A, which has an X-ray luminosity of 3.0×10^{44} ergs s^{-1} between 0.5 and 4.5 keV, and core radius 0.19 Mpc (Fabbiano *et al.* 1979).

These X-ray properties of Hydra A allow for its classification as a cooling flow cluster (Sarazin 1986). David *et al.* (1990) infer the mass flux to be 600 ± 120 $M_\odot$ yr^{-1} from the X-ray data. Other lines of evidence possibly supporting the cooling flow interpretation are the strong extranuclear line emission reported by Simkin (1979) and by Baum *et al.* (1988). Brightest cluster galaxies in strong cooling flows, like the Hydra A galaxy, have been found to have excess nonnuclear emission-line luminosities compared with typical radio galaxies of the same radio power (Heckman *et al.* 1989).

III. CALIBRATION AND DATA REDUCTION

Multiconfiguration observations of Hydra A were carried out at 4635, 4885, 14915, and 14960 MHz. The 14915 and 14960 MHz data in all configurations were combined because the change in polarization angle is less than 5° for a RM of 36,000 radians m^{-2}, far in excess of the maximum RM we believe likely in Hydra A. Table 2 contains a summary of the observations.

For gain calibration the standard VLA calibrators 3C 48 and 3C 286 were observed, usually at the beginning and the end of an observing run. Polarization and complex gain calibration were performed by observing the unresolved nearby source 0859−140 every half-hour for about 4 minutes at each frequency band. After calibration, all data reduction was performed using the NRAO Astronomical Image Processing System (AIPS), using the standard techniques.

The resulting cleaned 6 cm intensity maps provide 0″.6 resolution and an rms noise of 0.39 mJy $arcsec^{-2}$, giving a dynamic range of ~ 1300. The Stokes parameter Q and U maps have noise 0.11 mJy $arcsec^{-2}$, comparable to the expected thermal noise. The 2 cm intensity map made from B-,

TABLE 2

VLA OBSERVATIONS OF HYDRA A

Date	Configuration	Frequencies (MHz)	Duration (hr)[a]	Bandwidth (MHz)
1987 Oct 8	A	4635, 4885	2.28	12.5
1987 Oct 30	A/B	4635, 4885	1.98	12.5
		14915, 14965	1.62	12.5
1987 Nov 18	B	4635, 4885	2.62	50
		14915, 14965	1.88	50
1988 May 8	C	4635, 4885	1.24	25
		14915, 14965	2.38	25
1988 Aug 14	D	1465, 1515	0.36	50
		4635, 4885	0.38	50
		8435, 8785	0.52	50
		14915, 14965	2.62	50
1989 Jan 11	A	4635, 4885	3.13	25
		14915, 14965	2.65	25

[a] Time spent on source with each IF pair.

C-, and D-configuration data at 0".6 resolution has an rms noise of 0.29 mJy arcsec^{-2}, giving a dynamic range of $\sim$1900. The Q and U maps have noise 0.20 mJy arcsec^{-2}.

Making multiconfiguration data sets has the advantage of increasing the resolution possible without giving up sensitivity to large-scale features in the map. Some errors will result, however, if the intensity of the radio source varies between observations. Hydra A has an unresolved active core. Many of these core sources have proved to be variable in intensity over a period of months. Our observations ran over many months, so it was necessary to check for core variability. The results listed in Table 3 show that the core of Hydra A was variable by less than 15% at 2 cm over the time observed. These variations are considerably larger than errors resulting in flux bootstrapping, which should be good to $\sim$5%. No correction was made for any errors this may have introduced into the mapping process, since the resulting errors are below the thermal noise.

IV. TOTAL INTENSITY MAPS

a) Large-Scale Structure

At 6 cm and 0".6 resolution the bright central region of Hydra A is visible extending symmetrically about 45" (69 kpc) in both the northeast and southwest directions (Fig. 1). Observations in the D-configuration with the 20 cm band (50" resolution) show extended emission in the far north region out to 5' (420 pc) from the radio core (see Fig. 2). Overall, Hydra A extends about 8' (670 pc) in the north-south direction and 4' (335 kpc) in the east-west direction. Twin jets are visible emanating from the core. These jets appear to flare abruptly into the radio lobes at about 7" (10 kpc) from the core. A clear hotspot appears in the southern lobe, but no such clear indicator of the end of the jet is evident in the northern lobe. The southern lobe also shows an oscillation along the southern edge with a wavelength of 3".5 ± 1".1 and an amplitude of 0".5 ± 0".2.

TABLE 3

CORE VARIABILITY AT 2 CENTIMETERS

Date	Configuration	Peak Core Flux Density (Jy)
1987 Oct 30	A/B	0.236
1987 Nov 18	B	0.229
1988 May 8	C	0.237
1988 Aug 14	D	0.222
1989 Jan 11	A	0.253

Hydra A is edge-darkened, classifying it as a Fanaroff-Riley (1974) type I (FR I) source. The spectral radio luminosity at 178 MHz, however, we estimate to be $P_{178} = 3 \times 10^{26}$ W Hz^{-1} sr^{-1} (assuming a spectral index of 0.9; see § V), which is more characteristic of the edge-brightened FR II sources. The observed break between the two types is near 2×10^{25} W Hz^{-1} sr^{-1}, so Hydra A is 10 times too luminous for its morphology. Such overluminous type I sources are very rare, perhaps the best-known other example being Hercules A (3C 348) (Dreher and Feigelson 1984).

b) Jets

The jets display rotational, or "S" symmetry from the radio core into the lobes. This inner region is shown in Figure 3 at 0".6 resolution. Some peculiar features visible at low intensity, such as the hooklike structure near the core, are not real and are due to small residual phase errors. The width and brightness of the jets were estimated by fitting Gaussians to the intensity profiles at 0".6 resolution at several locations (the crosses in Fig. 3) in both jets. Some typical intensity profiles are shown in Figure 4. The northern jet brightens from 10 mJy arcsec^{-2} to 100 mJy arcsec^{-2} at a distance of 5" (7 kpc) from the core, whereas the southern jet is at all places below 10 mJy arcsec^{-2} (Fig. 5).

Assuming that the intrinsic intensity profile of the jet is Gaussian, then the intrinsic FWHM of the jet, σ_w, can be found by deconvolving the beamwidth, σ_b, from the jet profile by

$$\sigma_w = (\sigma_m^2 - \sigma_b^2)^{1/2} , \qquad (2)$$

where σ_m is the measured FWHM of the Gaussian fit to the jet. The apparent and deconvolved FWHMs for the jets are plotted against distance from the core in Figure 6.

V. SPECTRAL INDEX

The spectral index α (defined by $S_\nu \propto \nu^{-\alpha}$) of Hydra A from single-dish observations (Kühr *et al.* 1981) from 100 MHz to 10 GHz is 0.93. This value is much steeper than the median value of 0.73 predicted by the bivariate relation of Windhorst,

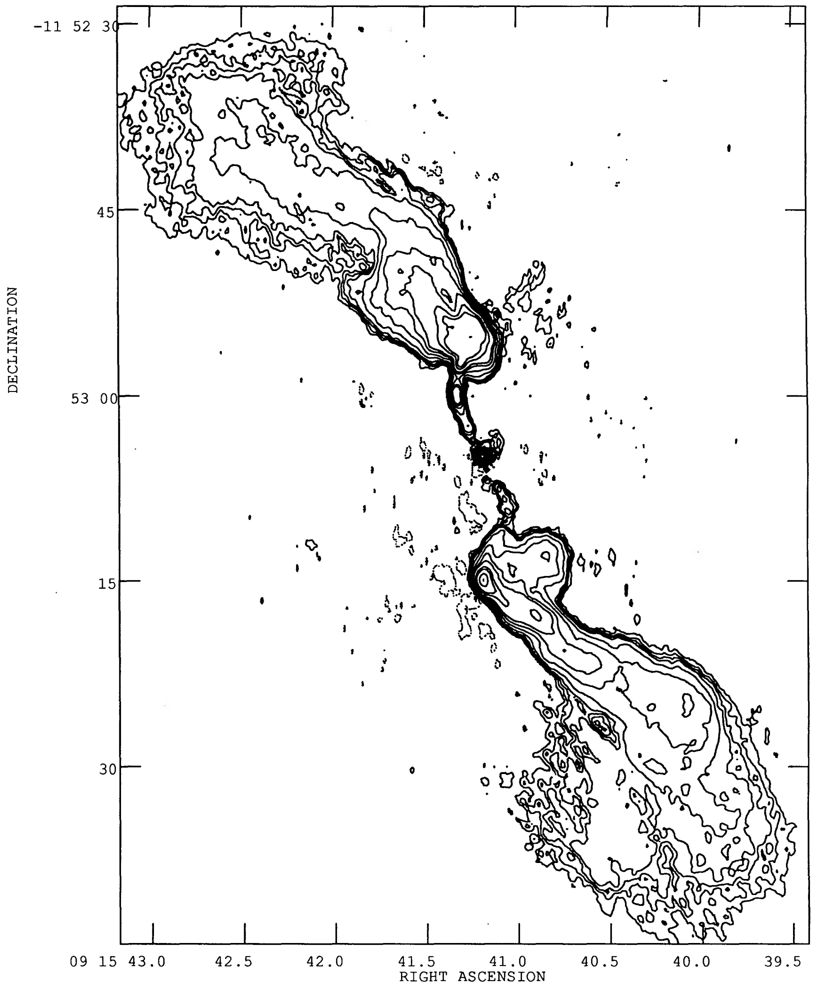

FIG. 1.—Total intensity distribution of Hydra A at 4635 MHz from A-, A/B-, B-, C-, and D-configuration data at 0".6 resolution. Contour levels are at −3.7, −1.5, 1.5, 2.7, 3.7, 5.1, 10, 21, 37, 51, 103, 154, 311, and 466 mJy arcsec^{-2}, with negative contours shown as dashed lines.

Mathis, and Neuschaefer (1989) for a source with the redshift and luminosity of Hydra A.

Figure 7 shows a 1".2 resolution map of the spectral index made from total intensity maps at 4635 MHz and at the averaged 2 cm frequency of 14940 MHz. In the lobes the spectral index steepens with distance from the core, reaching $\alpha = 2.0$ in places. This steepening, which is indicative of the aging of the relativistic electron spectrum, can be used to calculate a flow velocity in the lobes, following the procedure outlined in Myers and Spangler (1985). Assuming an initial power-law distribution of electron energies with $\gamma = 2.5$, that the steepening of the radio spectrum is entirely due to synchrotron losses, and that no reacceleration of electrons occurs in the lobes, the flow velocity can be determined. The southern lobe has a well-defined hot spot with $\alpha = 0.73 \pm 0.13$, and extends about 25" (35 kpc), where it reaches $\alpha = 1.50 \pm 0.10$. Figure 8 shows a slice along the axis of the southern lobe. Assuming a constant magnetic field strength equal to the minimum energy magnetic field strength of 17.5 μG (see § VI), we find $v_s = 9200$ km s^{-1}.

The presence of a far northern component to Hydra A that is visible only in the 20 cm map (Fig. 2), and not in the 6 cm map at the same resolution, indicates an extremely steep spectrum at large distances from the core. The brightness of this northern component is 0.075 mJy arcsec^{-2}. Assuming that this northern extension would be visible if it were 2 or more times the noise in the 6 cm map at the same resolution (rms noise = 0.003 mJy arcsec^{-2}) yields a spectral index greater than or equal to 2.15. The steepness of this result indicates that the far northern extension is quite old. The age in millions of years, $t_{\rm Myr}$, can be calculated from Myers and Spangler (1985) by

$$t_{\rm Myr} = 1060\left[\frac{X_0}{(1+z)\nu_{\rm GHz} B_{\mu \rm G}^3}\right]^{1/2}, \tag{3}$$

where $B_{\mu \rm G}$ is the effective magnetic field in μG and X_0 is a model-dependent function of the observed spectral index, frequencies, and initial spectral index. The minimum energy magnetic field strength, $B_{\rm me}$, in the far northern region is 6.5 μG (see § VI), about twice that of the equivalent cosmic microwave background magnetic field, $B_{\rm cmb} = 3.4(1+z)^2$ μG, assuming a current temperature of 2.8 K for the microwave background. The effective magnetic field for synchrotron and inverse Compton losses, $B_{\mu \rm G}$, can be calculated (Alexander and Leahy 1987)

$$B_{\mu \rm G}^3 = \frac{(B_{\rm me}^2 + B_{\rm cmb}^2)^2}{B_{\rm me}}. \tag{4}$$

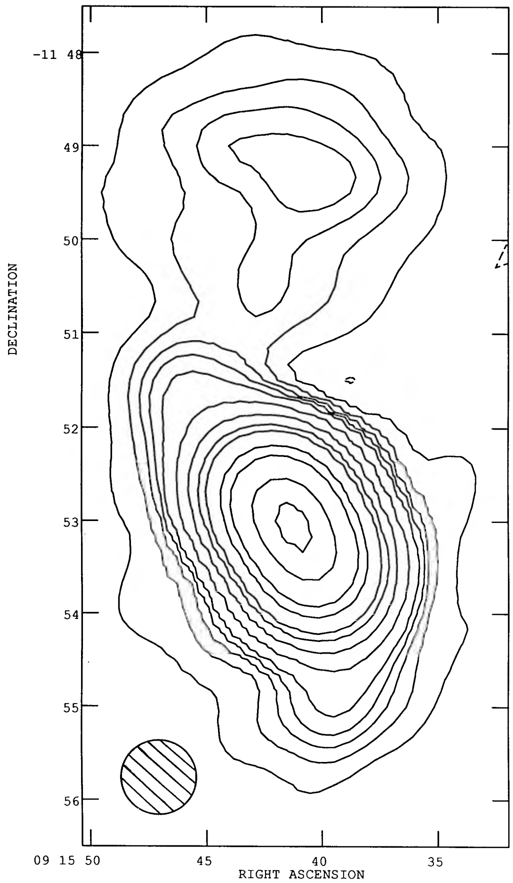

FIG. 2.—Total intensity distribution of Hydra A at 1465 MHz from D-configuration data at 50″ resolution. The beam size is shown in the lower left-hand corner. Contour levels are at −0.0085 (*dashed*), 0.0085, 0.025, 0.042, 0.060, 0.085, 0.17, 0.34, 0.60, 0.85, 1.7, 2.5, 4.9, and 7.8 mJy arcsec^{-2}.

Assuming an initial spectral index of 0.75 and constant pitch-angle scattering of the radiating electrons gives an age of 47 Myr. To have arrived at a distance of 5′ (420 kpc) in this time would require a velocity of 8800 km s^{-1}, comparable to the velocity derived from the spectral index gradient of Figure 8. A simple model of the radio lobes as chimneys of buoyantly rising plasma in a constant pressure gradient yields a velocity for the rising gas of

$$v = c_s \left(\frac{2\Delta\rho_{\rm ext}}{\rho_{\rm int}} \right)^{1/2} , \quad (5)$$

where c_s is the speed of sound in the external medium, $\Delta\rho_{\rm ext}$ is the change in density in the external medium, and $\rho_{\rm int}$ is the density of the lobe material. After obtaining c_s and $\Delta\rho_{\rm ext}$ from X-ray observations (David *et al.* 1990), we find that a lobe density of 2.2×10^{-4} cm^{-3} can produce a flow velocity of 9000 km s^{-1}, consistent with our spectral index observations.

VI. MINIMUM ENERGY MAGNETIC FIELDS AND PRESSURES

In Table 4 we show the minimum energy magnetic fields, energy densities, and pressures at selected points in the jets and lobes of Hydra A. These pressures and densities were calculated using the well-known assumption of minimum energy (Pacholczyk 1970; Miley 1980). Provided that the filling factor is unity, the pressures listed are true minima. Recent high-resolution observations, however, reveal the presence of filaments in many radio sources (e.g., Cygnus A, Perley, Dreher, and Cowan 1984; several wide-angle tail sources [WATs], O'Donoghue 1989) indicating a filling factor less than 1 in places, but estimates for this factor vary. We have assumed a cylindrical source geometry (Perley, Willis, and Scott 1979), equal energies in electrons and protons such that $k = 1$, and that the radio jets and lobes all lie in the plane of the sky. If the last assumption is invalid, then Doppler beaming effects must be taken into account if the lobe or jet velocities are close to c.

Taylor and Wright (1989) found that a hot IGM with electron density $n_e = 6.3 \times 10^{-7}$ cm^{-3} and temperature $T_0 = 10$ keV (1.2×10^8 K) could reproduce both the observed X-ray background and the observed distortion of the cosmic microwave background. This gives a gas pressure for the IGM of 2.1×10^{-14} dynes cm^{-2} well away from any cluster. In the far northern steep-spectrum lobe at 4′ (335 kpc) from the core, we find the minimum pressure about an order of magnitude greater than the thermal pressure of the IGM. The IGM pressure around the far northern lobe is probably enhanced by a higher density and could well be in pressure balance with the radiating plasma. Using the density profile predicted by the X-ray observations (eq. [1] of David *et al.* 1990), we get $n_{\rm H} = 0.001$ cm^{-3} at 4′ (335 kpc) separation. Taking their temperature of 4.5 keV and assuming a standard composition of 9 hydrogen nuclei and 1 helium nucleus for every 11 electrons, we find a total gas pressure of 1.6×10^{-11} dynes cm^{-2}, an order of magnitude higher than the minimum energy pressure of the far northern lobe. Since the gas pressure is derived from an azimuthally averaged density profile, clumping of the gas would allow the presence of lower pressure regions.

The gas pressure within the central region from the observations of David *et al.* (1990) is 1.0×10^{-10} dynes cm^{-2}, somewhat larger than the minimum pressure of the inner radio lobes but less than the minimum pressure of the jets. In general, the minimum pressure of the radiating plasma falls faster with distance from the core than the thermal pressure of the ICM. The jets, with their high brightness and small emitting volume, have the highest pressures, and may not yet have had time to

TABLE 4

MINIMUM ENERGY MAGNETIC FIELD STRENGTHS AND PRESSURES

Site	Emissivity (ergs s^{-1} sr^{-1} cm^{-3})	$B_{\rm me}$ (μG)	$U_{\rm me}$ (ergs cm^{-3})	$P_{\rm me}$ (dynes cm^{-2})
Far N lobe	1.00×10^{-29}	6.53	3.96×10^{-12}	1.32×10^{-12}
N lobe	6.06×10^{-28}	17.5	2.83×10^{-11}	9.46×10^{-12}
N jet knot	1.18×10^{-25}	69.4	4.47×10^{-10}	1.49×10^{-10}
N inner jet	1.29×10^{-26}	36.8	1.26×10^{-10}	4.19×10^{-11}
S jet	6.06×10^{-27}	29.9	8.29×10^{-11}	2.77×10^{-11}
S lobe	6.06×10^{-28}	17.5	2.83×10^{-11}	9.46×10^{-12}

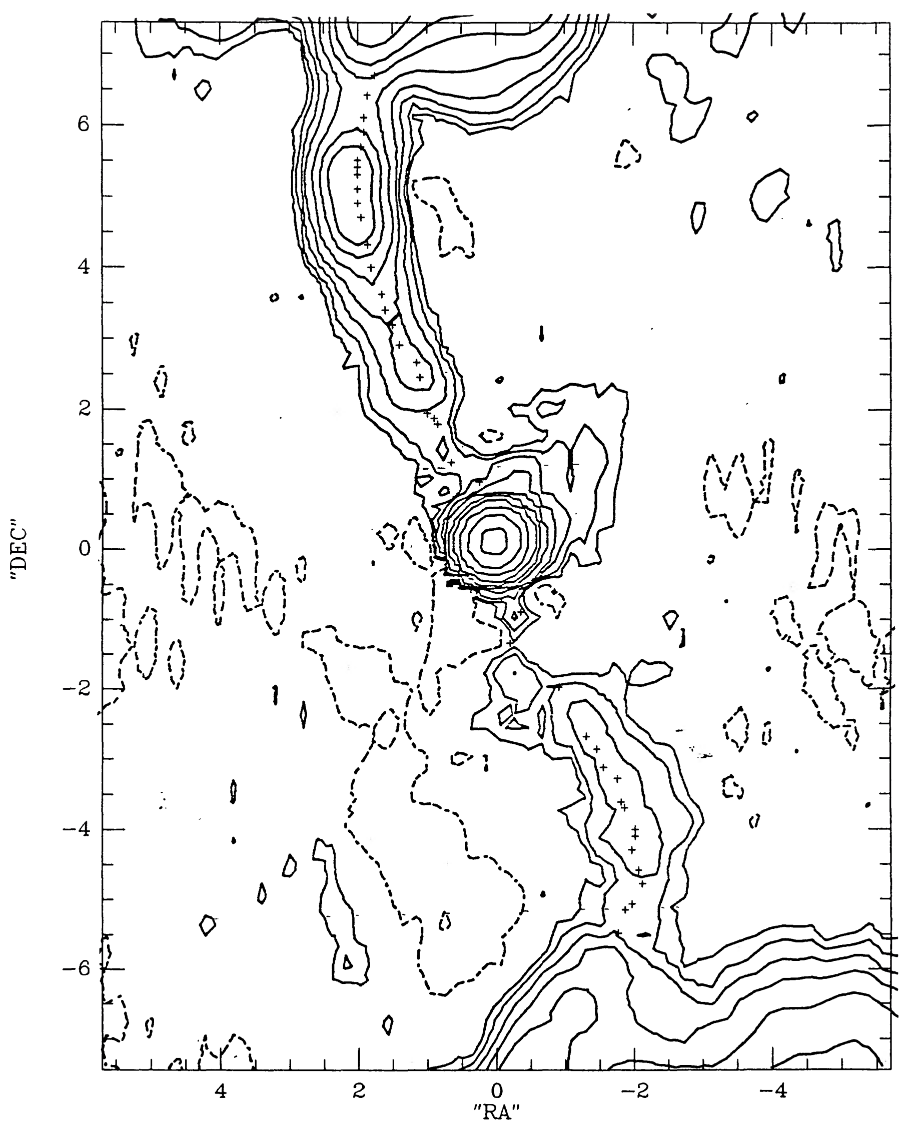

FIG. 3.—Enlargement of the central region of Fig. 1. Contour levels are −1.0 (*dashed*), 1.0, 2.0, 7.8, 15, 32, 51, 103, 208, and 417 mJy arcsec^{-2}. The plus signs represent locations where a Gaussian was fitted to the jet. The hooklike feature near the core is the result of phase errors.

achieve equipartition or minimum energy. The jets are also barely resolved, and in fact the deconvolved FWHM size used may not be entirely accurate. A smaller jet width, s, will increase the pressure in the jets, since $P_{\rm me} \propto s^{-4/7}$.

VII. ROTATION MEASURES

An electromagnetic wave traveling through an electron-ion plasma along a magnetic field will undergo a rotation of its plane of polarization (Burn 1966) according to

$$\psi = \psi_0 + \frac{e^3}{2\pi m_e^2 c^4} \lambda^2 \int_0^L n_e B_{\parallel} \, dl = \psi_0 + {\rm RM}\lambda^2 , \qquad (6)$$

where ψ_0 is the initial polarization angle and RM is the rotation measure. Evaluating the constants in equation (6) gives

$${\rm RM} = 812 \int_0^L n_e B_{\parallel} \, dl \ {\rm radians\ m^{-2}} , \qquad (7)$$

where $B_{\parallel}$ is measured in μG, n_e in cm^{-3}, and dl in kpc.

The RMs in Hydra A were determined from the 4635, 4885, and 14915 MHz 0."6 resolution maps at each pixel independently by performing a weighted linear least-squares fit to a plot of ψ versus λ^2. No value was determined for a given pixel unless the errors in ψ at all frequencies were less than 10°. A few sample calculations of the RM in the northern lobe are shown in Figure 9. Calculations throughout the northern lobe (Fig. 10) show RMs ranging from −1000 to +3300 radians m^{-2}. Several regions with diameters ~3" (4.2 kpc) show roughly homogeneous RMs indicating that the magnetic field producing them is ordered on this scale. A rotation of the polarization angle of +180° between the two frequencies in the 6 cm band corresponds to a RM of +7500 radians m^{-2}, so the RMs in the northern lobe approach the maximum values, ±3750 radians m^{-2}, that can be determined unambiguously by these observations. Gradients in the RM of 1000 radians m^{-2} over 1" are observed in the northern lobe. The 2 cm data are ~50% polarized in the northern lobe, while the 6 cm data are ~40% polarized. Mechanisms for producing such large RMs will be discussed in § IX.

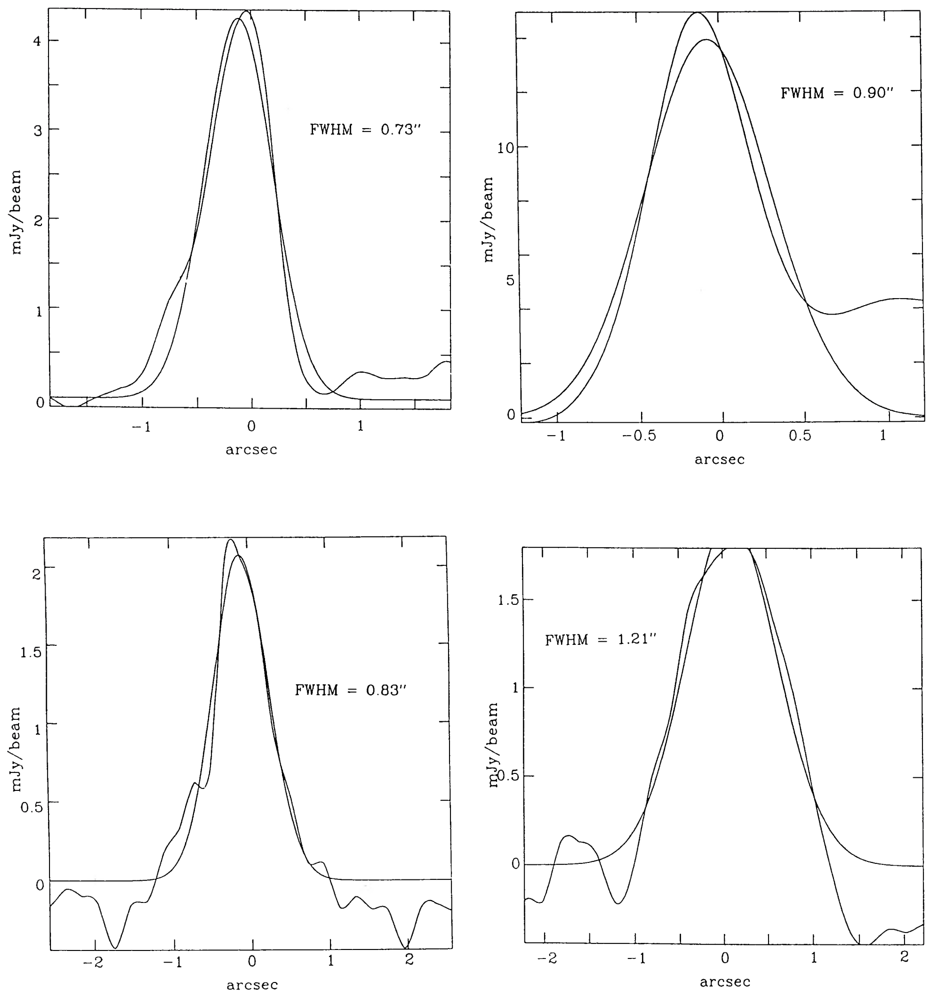

FIG. 4.—Some sample slices and Gaussian model fits for the plus signs in Fig. 3. The top pair is from the northern jet, and the bottom pair from the southern jet.

Large gradients in the RM cause severe beamwidth depolarization at low frequencies. In the southern lobe the degree of polarization at 6 cm is $\sim 2\%$. The RM map, where the RM can be determined, shows many flips in the RM indicating the presence of $n\pi$ ambiguities in the data, which in turn suggests RMs in excess of ± 3750 radians m^{-2} (Fig. 11). Unambiguous determinations of RM require two frequencies sufficiently close that the change in position angle is less than $\pm 90°$. Other frequencies are needed to judge whether this condition is met, and to improve the accuracy of the RM calculations, especially if the range in RMs is large. The flips observed in the southern lobe tell us that the above condition was not met between 4635 and 4885 MHz, allowing for multiple solutions (see Fig. 12). These RMs are sufficient to explain the low polarization at 6 cm through beamwidth depolarization.

The larger RMs present in the relatively unjetted, southern side may be due to the inclination of the source to the line of sight, which is such that the south side is farther away, so it is seen through a deeper Faraday screen causing more depolarization. This supports the finding of Laing (1988) that the side of the stronger jet of radio galaxies and quasars shows less depolarization. Garrington *et al.* (1988), in a follow-up survey, found that 23 out of 25 FR II sources show less depolarization on the jetted side. This would indicate that radio lobes in these sources are frequently surrounded by a magnetized plasma and that Doppler beaming is responsible for the apparent one-sidedness of their jets.

VIII. MAGNETIC FIELD CONFIGURATION

Once the RM at a specific point has been determined by a fit to a plot of the polarization angle versus λ^2, the intrinsic electric field polarization angle of the emitting plasma, ψ_0, can be found by extrapolating back to zero wavelength. Adding 90° to this value gives the orientation of the magnetic field. Figure 13 shows the projected magnetic field configuration in Hydra A. The length of the vectors represents the fractional polarization at 2 cm, and the contours come from the total intensity map at 2 cm. For the most part, the field configuration follows the edges of the source as has been observed in many extragalactic radio sources (e.g., Cygnus A, Dreher, Carilli, and Perley 1987, hereafter DCP; 3C 219, Perley *et al.* 1980; NGC 6251, Perley, Bridle, and Willis 1984). This is true to a lesser extent in the southern lobe, where the magnetic field is not as well ordered as in the northern lobe and many erroneous RMs are likely. The magnetic field in the northern jet is predominantly parallel to the jet axis, like that of many one-sided powerful FR II sources (Bridle and Perley 1984), but unlike normal FR I sources. In 3C 83.1B (NGC 1265), where O'Dea and Owen (1987) find both parallel and perpendicular field configurations, they attribute the parallel fields to shearing effects.

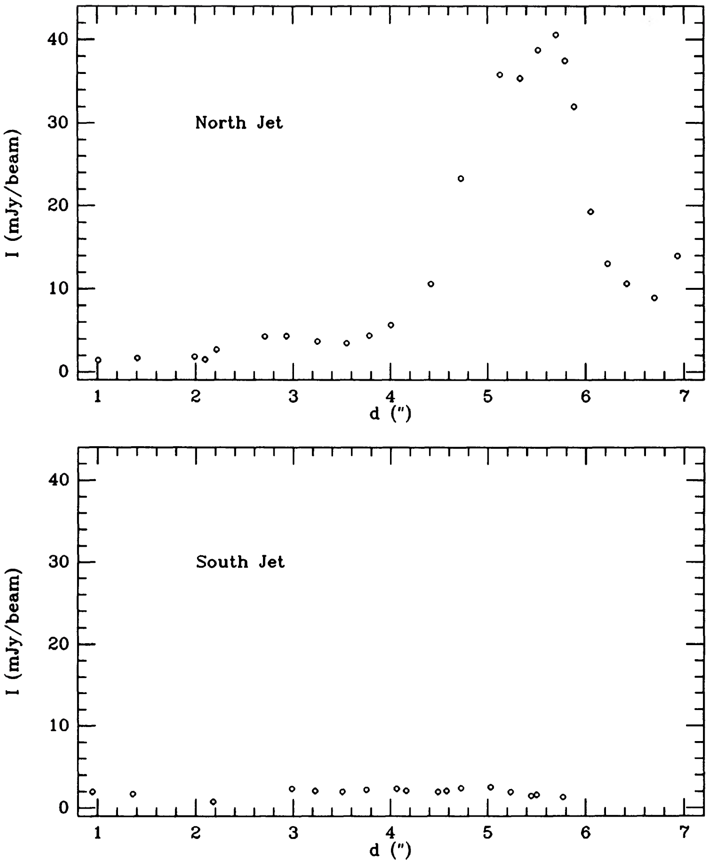

FIG. 5.—Plots of intensity vs. distance from the core for the northern (*top*) and southern (*bottom*) jets.

This agreement of the field configuration in Hydra A with similar results in other extragalactic radio sources reassures us that we have correctly measured the RM structure. Better data, such as we hope to obtain at 3.6 cm, would allow us to map better the southern magnetic field configuration and see whether, for example, the magnetic field configuration follows the oscillations visible along the southern edge of Hydra A.

IX. DISCUSSION

a) Precession of the Jets

The standard model for the production of twin radio jets is a massive black hole accreting material in the nucleus of a galaxy and pumping a good fraction of the energy released into the radio lobes through these narrow beams of relativistic plasma (Begelman, Blandford, and Rees 1984). Rees (1978) argues that these jets are collimated close to the black hole and therefore emerge along its spin axis due to the Lense-Thirring effect from a rotating black hole. If this is indeed the case, then a precession of the black hole would result in a precession of the jets. The black hole, with mass M, can be made to precess in a suitable gravitational field, such as that from another, orbiting, black hole of mass m. In a wide binary system, by a straightforward application of Kepler's third law, the orbital period is

$$P_{\rm orb} \approx 1.6 r_{16}^{3/2} M_8^{-1/2}\ {\rm yr}\ , \tag{8}$$

where r_{16} is the orbital separation in units of 10^{16} cm and M_8 is the mass of the larger black hole in units of $10^8\ M_\odot$. The period of precession about the angular momentum axis of the orbit for the more massive black hole is given by Begelman, Blandford, and Rees (1980) as

$$P_{\rm prec} \approx 600 r_{16}^{5/2} M_8^{-3/2} (M/m)\ {\rm yr}\ . \tag{9}$$

The presence of a secondary optical nucleus 10″ from the primary nucleus in Hydra A suggests that a merger of two galaxies occurred. The smaller black hole could then have settled out under dynamical friction to orbit the more massive active black hole. The position of the secondary nucleus in the plane of rotation of the gas and stars (Ekers and Simkin 1983), lends credence to this scenario.

The inversion symmetry of the radio jets in Hydra A is suggestive of precession. Gower *et al.* (1982) present kinematical models for the geometry and intensity of twin precessing jets, taking into account the effects of Doppler beaming and projection onto the plane of the sky. Comparison of these models by Gower *et al.* with three radio galaxies gave periods of $\sim 10^6$ yr and jet velocities of 0.2c. The jets of Hydra A possess a clear wobble, rotation-symmetric about the core, with a wavelength of about 20″ (28 kpc). Assuming that the velocity in the lobes is 10^4 km s^{-1} from spectral index gradient measurements, and that the jet velocity is between this velocity and c, then 10^5 km s^{-1} seems a reasonable jet velocity, and gives a precession period of $\sim 3 \times 10^5$ yr. With this period, $M_8 = 1$, and $m_8 = 0.1$, equation (9) gives $r_{16} = 4.8$, or approximately 3200 AU for the orbital separation.

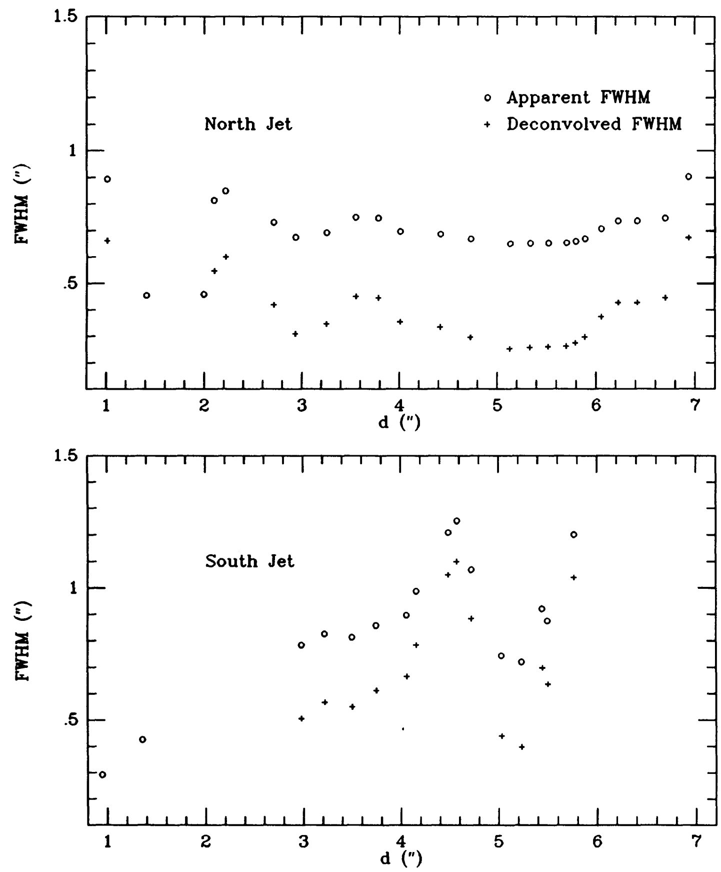

FIG. 6.—Plots of the apparent and deconvolved full width at half-maximum (FWHM) of the northern and southern jets against distance from the core. The apparent FWHM is measured from the Gaussian fits to the jet.

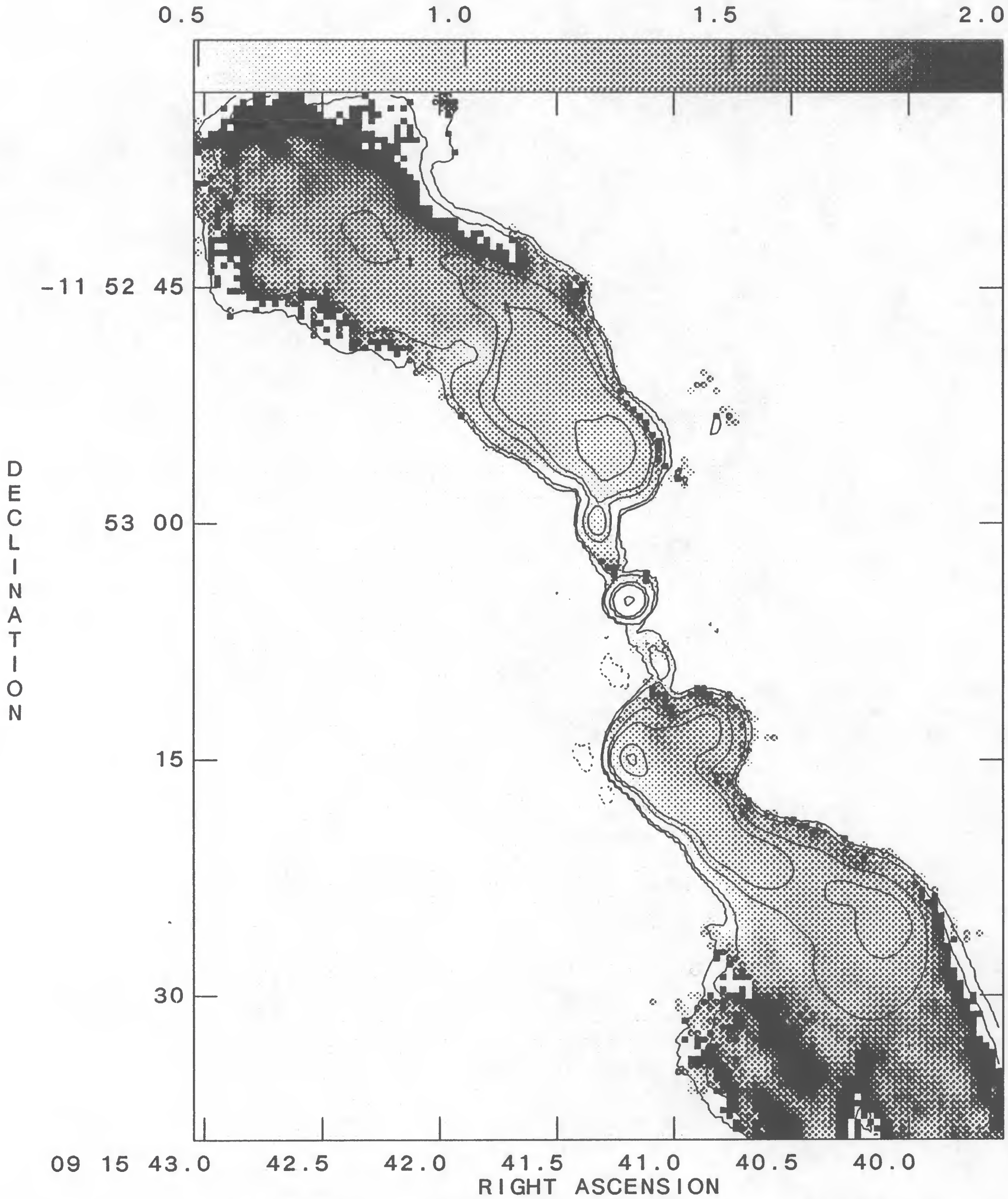

FIG. 7.—Spectral index of Hydra A calculated from the 14940 and 4635 MHz 1".2 resolution maps. Contours from the 4635 MHz data are overlaid at −2.4, −1.2, 1.2, 2.4, 12, 24, 120, and 216 mJy arcsec^{-2}.

b) The Faraday Rotating Medium

Typical extragalactic sources at high Galactic latitude have RMs on the order of 0–100 radians m^{-2} in absolute value induced by the passage of their radiation through the ISM of our Galaxy, with sources at low Galactic latitudes possessing larger RMs (Inoue and Tabara 1981; Simard-Normandin, Kronberg, and Button 1981). Hydra A has a Galactic latitude of 25°.1, and the observed RMs are at least an order of magnitude too large to be produced along the line of sight within our Galaxy.

The Faraday rotation of Hydra A could be produced within the source by the magnetic field and density there, although it would be hard to explain the observed RM asymmetry between the northern and southern lobes by this model. Consider a simple slab model with constant density and magnetic field. For a path length of 20" (28 kpc) through the southern lobe, taking the minimum energy value of 18 μG as an estimate of the magnetic field strength, to achieve a RM of 4000 radians m^{-2} requires an electron density of ~ 0.02 cm^{-3}, comparable to that of the external medium. Several groups, including DCP and Laing and Bridle (1987), have attempted to measure the density in lobes and jets by examination of RMs and estimates of the magnetic field strength. If the Faraday RMs were produced within the jets and lobes, then we would expect to observe a large amount of depolarization at low frequencies. The combination of electron density and magnetic field strength given above gives 95% depolarization at 6 cm due to differential Faraday rotation from the back to the front of the

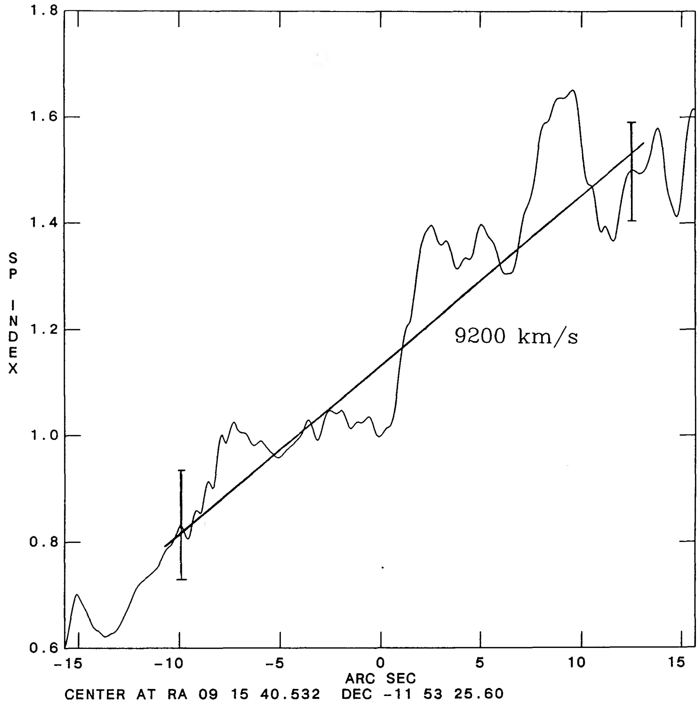

FIG. 8.—Slice of the spectral index from Fig. 7 going from the southern hot spot toward the edge of the lobe along the lobe axis. Two sample error bars are shown. The slope of the solid line corresponds to a velocity of 9200 km s^{-1} as derived in the text.

If an intracluster magnetic field is responsible for the observed RMs, then it must be at least 3 μG. This requires an energy density comparable to that of the microwave background, and a total energy in the cluster magnetic field of 3.5×10^{59} ergs. Although considerable, this energy in the magnetic field is still two orders of magnitude less than the thermal energy of the hot cluster gas. The origin of this magnetic field is not known. One interesting possibility suggested by DCP comes from the idea that cD galaxies in cluster centers, like Hydra A, are thought to have achieved their large size by cannibalizing some of their fellow galaxies. The magnetic fields of these eaten galaxies might then remain spread around the cluster center like ghosts. Ruzmaikin, Sokoloff, and Shukurov (1988), extending earlier work by Jaffe (1980), have discussed the possibility that turbulent motions in galaxy wakes can amplify seed fields sufficiently to produce RMs of 4000 radians m^{-2}.

Recently, Bicknell, Cameron, and Gingold (1990), have suggested that the high RMs observed in Cygnus A result from mixing of the cluster gas with the magnetic field of the radio source. In Hydra A this would result in a very low percentage polarization at 6 cm *throughout* the source compared with that at 2 cm. This low percentage of polarized emission is seen in the southern lobe but not in the northern lobe. We believe the low percentage of polarized emission in the southern lobe is due to transverse Faraday effects. A gradient of 1000 radians m^{-2} $arcsec^{-1}$ will rotate a 4635 MHz wave by 144° across a 0."6 beam. In Hydra A these gradients are so large as to have severely depolarized the 6 cm data, especially in the southern lobe where the RMs and the gradients in RM are larger. We await the arrival of the higher resolution, higher frequency observations at 3.6 cm in order to attempt to calculate the amount of depolarization, if any, occurring as a result of internal Faraday rotation.

The most likely source of RM seems to be from an extensive ($\sim$200 kpc in radius) external screen around Hydra A. The screen needs to be of this size (greater than the size of the source) in order to provide similar magnitude RMs around the lobes as well as the jets. Assuming a simple slab model in which $n_e = 0.008$ cm^{-3} (the central electron density from X-ray observations), with $B_{\parallel}$ constant throughout, and taking 200 kpc for the path length through the slab, allows us to solve equation (7), yielding $B_{\parallel} = \mathrm{RM}/1280$ μG with the RM expressed in radians m^{-2}. So for a RM = 4000 radians m^{-2}, $B_{\parallel} = 3.1$ μG. This provides a minimum estimate of the magnetic field outside Hydra A, since field reversals would cause us to underestimate the magnetic field.

Following DCP, integrating the density profile from X-ray observations yields $B_{\parallel} = 3.6$ μG. The magnetic field may not be constant with distance from the core. Assuming that it scales as $n^{1/2}$, if the magnetic field energy scales with the thermal energy, gives a central $B_{\parallel} = 3.8$ μG.

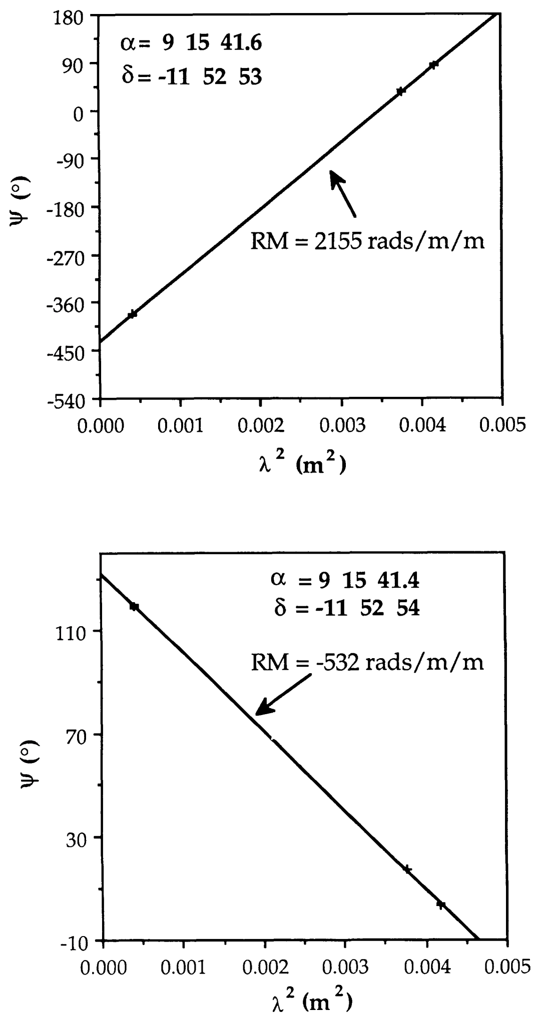

FIG. 9.—Sample fits of the polarization angle (ψ) against λ^2 from two pixels in the northern lobe. RMs were calculated independently at each pixel from the polarization angles at 4635, 4885, and 14915 MHz in the 0."6 resolution maps. The rms error for the top fit is 2°21, and for the bottom fit 0°90. Error bars for each point are plotted, but are generally smaller than the size of the point.

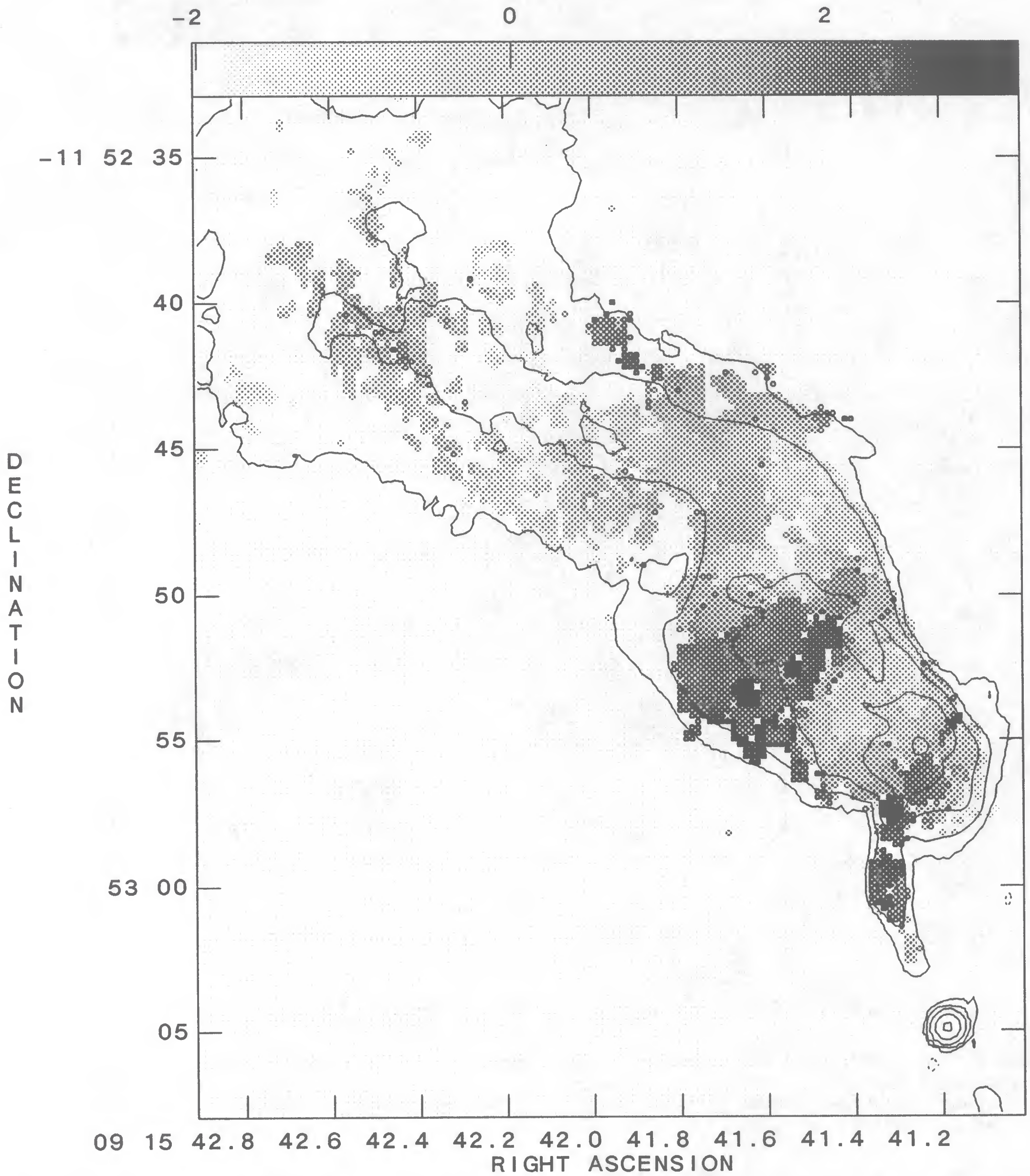

FIG. 10.—RM structure of the northern lobe of Hydra A. This map shows orderly transitions from regions of −1000 to +3000 radians m^{-2}. Several regions with nearly uniform RMs are seen over patches of size ∼3″. Contours from the 4885 MHz data are overlaid at −2.7 (*dashed*), 2.7, 10.8, 43.1, 162, and 485 mJy arcsec^{-2}. The gray scale indicates RMs from −2000 to +3200 radians m^{-2}.

source, forming a thin, depolarizing layer separating the two gases. The mixing process must preserve the (presumably) ordered magnetic field of the lobe, otherwise the resulting RM would not display the observed large-scale order. Our observations cannot rule out this model, but they do demand that the mixing process occur equally for the jets and lobes, since the observed RMs are the same for both. A simple interpretation of the model would predict considerable depolarization along the edges of the source, and an increase in RM with radial distance as the mixing layer deepens. Neither effect is observed, however; the depolarized edge will be difficult to detect because of its thinness, and the radial dependence of RM requires data at a lower frequency. These data are being taken.

c) *Cooling Flows in Clusters*

Hydra A may possess a strong cooling flow with an accretion rate of $\sim 600\ M_{\odot}\ \mathrm{yr}^{-1}$ (David *et al.* 1990). A simple isotropic inflow of mass toward the cluster core, such as that modeled by White and Sarazin (1987), will not affect the radio lobes. At a distance of 40″ (56 kpc) from the core the inflow velocity from the models of White and Sarazin is only ∼20 km s^{-1}. The resulting dynamical pressure of the inflow, ρv^2, is 5.5×10^{-14} dynes cm^{-2}, which is 160 times smaller than the minimum energy pressure calculated for the southern radio lobe (see Table 4).

Other dominant galaxies in "cooling flow" clusters, like

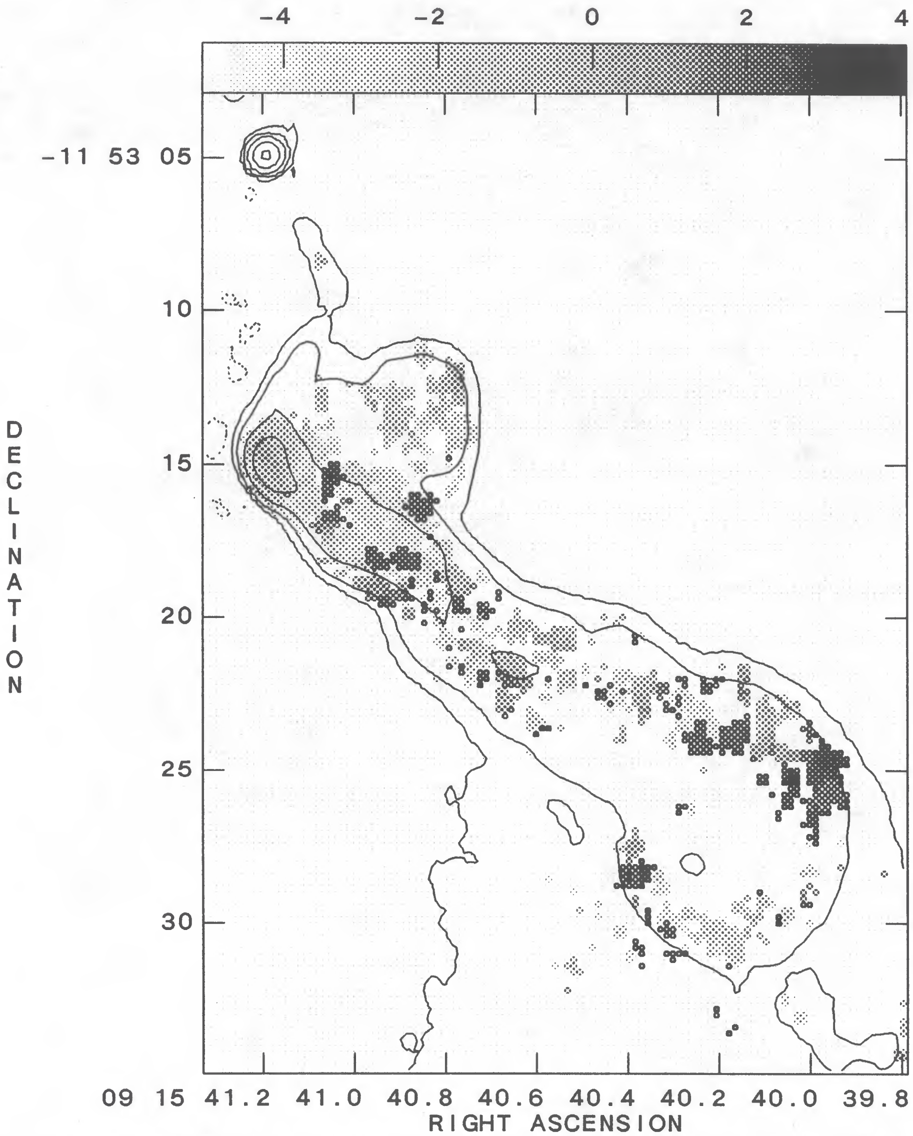

FIG. 11.—RM structure of the southern lobe of Hydra A. Note the abrupt transitions from +4000 to −4000 radians m^{-2}. These flips are indicative of RMs larger than we can unambiguously determine with our current observations. Gradients in RM appear much larger than in the northern lobe and have beamwidth-depolarized much of the 6 cm data. Contours from the 4885 MHz data are overlaid at −2.7 (*dashed*), 2.7, 10.8, 43.1, 162, and 485 mJy arcsec^{-2}. The gray scale indicates RMs from −5000 to +4000 radians m^{-2}.

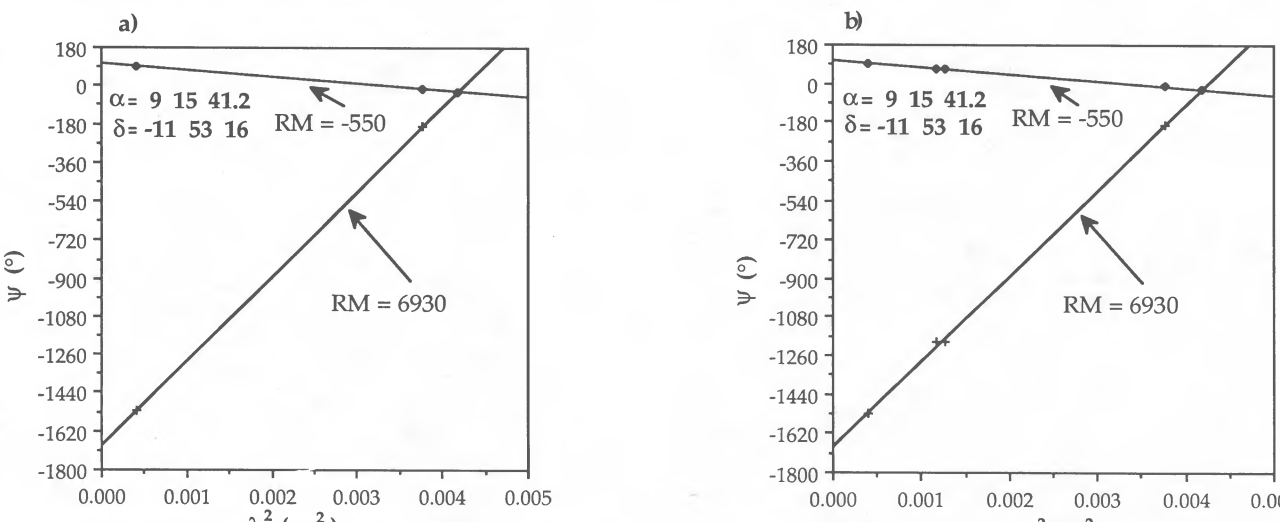

FIG. 12.—(*a*) Example of the RM ambiguities that are present in the southern lobe. Allowing for a rotation of ±180° between 4635 and 4885 MHz, a better fit can be obtained with RM = 6885 (rms = 0°62) than for the value RM = −550 (rms = 0°93). (*b*) Shows inclusion of 3.5 cm band frequencies at 8.44 and 8.79 GHz with values that fit the RM = −550 plot (rms = 0°62), do not fit the larger RM = 6930 fit (rms = 31°), and thus allow unambiguous determination of the RM.

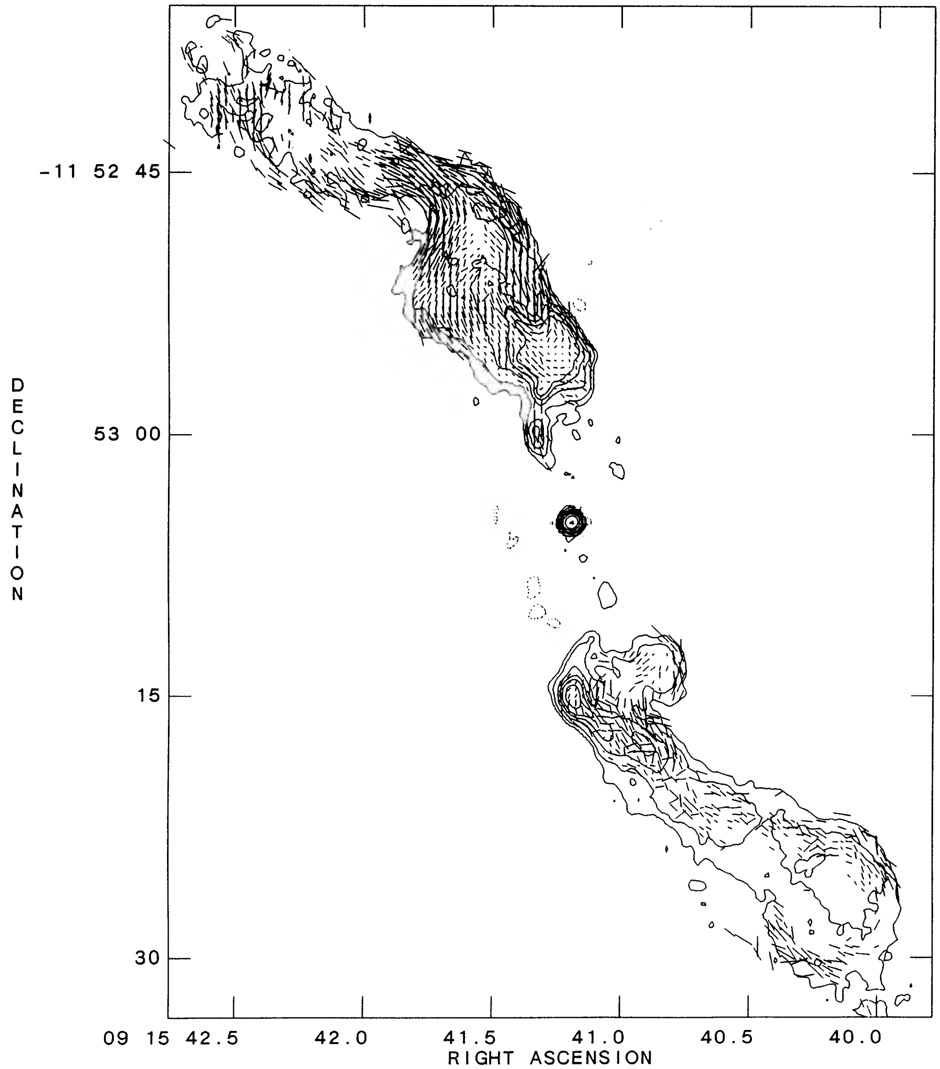

FIG. 13.—Magnetic field configuration in Hydra A corrected for the effect of RM. The length of the vector represents the percentage polarization at 2 cm (a 1″ length represents a 50% polarization), and contours from the 0″.6 resolution 2 cm data are overlaid at −2.16 (*dashed*), 2.16, 5.42, 16, 33, 54, 108, 216, and 488 mJy arcsec^{-2}.

Cygnus A (DCP; Carilli, Perley, and Dreher 1988) and 3C 295 (Perley and Taylor 1990), have powerful radio sources with high RMs. Perhaps the presence of a strong cooling flow, or the high central densities under which such a flow develops, helps create the dominant galaxy, strong radio emission, and high RMs. The cooling flow in Hydra A may be feeding the nuclear engine that powers the jets. It also seems likely that the large RMs result in part from the high density in the cluster, although the origin of the 3 μG cluster magnetic field is a mystery (if not a ghost story).

X. CONCLUSIONS

Hydra A is an FR I type radio galaxy of very high luminosity, even exceeding WATs in dense clusters, although similar to them in morphology. The minimum energy pressures for the radio lobes are an order of magnitude below the thermal pressures of the cluster gas. Observations of the spectral index variation in the lobes seem to indicate a drift speed of $\sim$9000 km s^{-1} and an age of $\sim 5 \times 10^7$ yr for Hydra A. We find that the "S" shape of the jets of Hydra A can be modeled by precession of the central engine (a supermassive black hole) due to another orbiting black hole. A period of $\sim 3 \times 10^5$ yr allows for many precessions over the lifetime of Hydra A, and requires a jet velocity of 100,000 km s^{-1}.

Our observations of the RM structure of Hydra A, combined with X-ray observations (David *et al.* 1990), indicate that Hydra A is embedded in a hot intracluster plasma of size $\sim$200 kpc, density 0.015 cm^{-3}, and magnetic field strength greater than 3 μG. Alternatively, the RM may be partially or wholly due to a mixing layer between the cluster and the radio source. Data to allow discrimination between these models are being taken. Hydra A, Cygnus A, and 3C 295 are all cD galaxies in high X-ray luminosity clusters showing ordered, extended RMs on kpc scales. Further studies of the RM structure of extended radio galaxies are needed to give insight about cluster environments and to define the relationship between X-ray emission, radio emission, cluster richness, and rotation measures.

G. B. T. would like to thank the University of California at Los Angeles and Mars, Inc., for support over the summer while staying at the VLA, where much of the data reduction was performed. G. B. T. also thanks the VLA staff for many helpful discussions.

REFERENCES

Abell, G. O. 1958, *Ap. J. Suppl.*, **3**, 211.
Alexander, P., and Leahy, J. P. 1987, *M.N.R.A.S.*, **225**, 1.
Baum, S. A., Heckman, T. M., Bridle, A. H., van Breugel, W. J. M., and Miley, G. K. 1988, *Ap. J. Suppl.*, **68**, 643.
Begelman, M. C., Blandford, R. D., and Rees, M. J. 1980, *Nature*, **287**, 307.
———. 1984, *Rev. Mod. Phys.*, **56**, 255.
Bicknell, G. V., Cameron, R. A., and Gingold, R. A. 1990, *Ap. J.*, **357**, 373.
Bridle, A. H., and Perley, R. A. 1984, *Ann. Rev. Astr. Ap.*, **22**, 319.
Burn, B. F. 1966, *M.N.R.A.S.*, **133**, 67.
Carilli, C. L., Perley, R. A., and Dreher, J. W. 1988, *Ap. J. (Letters)*, **334**, L73.
David, L. P., Arnaud, K. A., Forman, W., and Jones, C. 1990, *Ap. J.*, **356**, 32.
Dreher, J. W., Carilli, C. L., and Perley, R. A. 1987, *Ap. J.*, **316**, 611 (DCP).
Dreher, J. W., and Feigelson, E. D. 1984, *Nature*, **308**, 43.
Ekers, R. D., and Simkin, S. M. 1983, *Ap. J.*, **265**, 85.
Fabbiano, G., Doxsey, R. E., Johnston, M., Schwartz, D. A., and Schwartz, J. 1979, *Ap. J. (Letters)*, **230**, L67.
Fanaroff, B. L., and Riley, J. M. 1974, *M.N.R.A.S.*, **167**, 31P.
Fomalont, E. B. 1971, *A.J.*, **76**, 513.
Garrington, S. T., Leahy, J. P., Conway, R. G., and Laing, R. A. 1988, *Nature*, **331**, 147.
Gower, A. C., Gregory, P. C., Hutchings, J. B., and Unruh, W. G. 1982, *Ap. J.*, **262**, 478.
Heckman, T. M., Baum, S. A., van Breugel, W. J. M., and McCarthy, P. 1989, *Ap. J.*, **338**, 48.
Inoue, M., and Tabara, H. 1981, *Pub. Astr. Soc. Japan*, **33**, 603.
Jaffe, W. 1980, *Ap. J.*, **241**, 925.
Kato, T., Tebara, H., Inoue, M., and Aizu, K. 1987, *Nature*, **329**, 223.
Kühr, H., Witzel, A., Pauliny-Toth, I. I. K., Nauber, U. 1981, *Astr. Ap. Suppl.*, **45**, 367.
Laing, R. A. 1988, *Nature*, **331**, 149.
Laing, R. A., and Bridle, A. H. 1987, *M.N.R.A.S.*, **228**, 557.
Matthews, T. A., Morgan, W. W., and Schmidt, M. 1964, *Ap. J.*, **140**, 35.
Miley, G. K. 1980, *Ann. Rev. Astr. Ap.*, **18**, 165.
Morgan, W. W. 1958, *Pub. A.S.P.*, **70**, 364.
Myers, S. T., and Spangler, S. R. 1985, *Ap. J.*, **291**, 52.
O'Dea, C. P., and Owen, F. N. 1987, *Ap. J.*, **316**, 95.
O'Donoghue, A. A. 1989, Ph.D. thesis, New Mexico Institute of Mining and Technology.
Owen, F. N., and Laing, R. A. 1989, *M.N.R.A.S.*, **238**, 357.
Pacholczyk, A. G. 1970, *Radio Astrophysics* (San Francisco: Freeman).
Perley, R. A., Bridle, A. H., and Willis, A. G. 1984, *Ap. J. Suppl.*, **54**, 291.
Perley, R. A., Bridle, A. H., Willis, A. G., and Fomalont, E. B. 1980, *A.J.*, **85**, 499.
Perley, R. A., Dreher, J. W., and Cowan, J. J. 1984, *Ap. J. (Letters)*, **285**, L35.
Perley, R. A., and Taylor, G. B. 1990, in preparation.
Perley, R. A., Willis, R. G., and Scott, J. S. 1979, *Nature*, **281**, 437.
Rees, M. J. 1978, *Nature*, **275**, 516.
Ruzmaikin, A. A., Sokoloff, D. D., and Shukurov, A. M. 1988, preprint.
Sandage, A. 1973, *Ap. J.*, **183**, 731.
Sandage, A., and Hardy, E. 1973, *Ap. J.*, **183**, 743.
Sarazin, C. L. 1986, in *Proc. NRAO Workshop 16, Radio Continuum Processes in Clusters of Galaxies*, ed, C. P. O'Dea and J. M. Uson (Charlottesville: NRAO), p. 23.
Simard-Normandin, M., Kronberg, P. P., and Button, S. 1981, *Ap. J. Suppl.*, **45**, 97.
Simkin, S. M. 1979, *Ap. J.*, **234**, 56.
Taylor, G. B., and Wright, E. L. 1989, *Ap. J.*, **339**, 619.
White, R. E., and Sarazin, C. L. 1987, *Ap. J.*, **318**, 629.
Windhorst, R. A., Mathis, D., and Neuschaefer, L. 1989, in *The Evolution of the Universe of Galaxies* (Edwin Hubble Centennial Symposium), ed. R. Kron *et al.* (ASP Conf. Series; Provo: Brigham Young University), in press.

KO AIZU: Rikkyo University, Katahira 2-24-3, Asao-Ku, Kawasaki 215, Japan

MAKOTO INOUE: Nobeyama Radio Observatory, Nobeyama, Minamisaku, Nagano 384-13, Japan

TATSUJI KATO and HIROTO TABARA: Department of Education, Utsunomiya University, Mine, Utsunomiya 321, Japan

RICHARD A. PERLEY and GREGORY B. TAYLOR: NRAO, P.O. Box 0, Socorro, NM 87801